Competition Between Antiferromagnetic and Charge-Density-Wave Order in the Half-Filled Hubbard-Holstein Model

E. A. Nowadnick,[1,2] S. Johnston,[2,3,4] B. Moritz,[2,5,6] R. T. Scalettar,[7] and T. P. Devereaux[2]

[1]*Department of Physics, Stanford University, Stanford, California 94305, USA*
[2]*Stanford Institute for Materials and Energy Sciences, SLAC National Accelerator Laboratory and Stanford University, Stanford, California 94305, USA*
[3]*Institute for Theoretical Solid State Physics, IFW Dresden, Helmholtzstrasse 20, 01069 Dresden, Germany*
[4]*Department of Physics and Astronomy, University of Waterloo, Waterloo, Ontario N2L 3G1, Canada*
[5]*Department of Physics and Astrophysics, University of North Dakota, Grand Forks, North Dakota 58202, USA*
[6]*Department of Physics, Northern Illinois University, DeKalb, Illinois 60115, USA*
[7]*Department of Physics, University of California, Davis, California 95616, USA*

(Received 4 September 2012; published 10 December 2012)

We present a determinant quantum Monte Carlo study of the competition between instantaneous on-site Coulomb repulsion and retarded phonon-mediated attraction between electrons, as described by the two-dimensional Hubbard-Holstein model. At half filling, we find a strong competition between antiferromagnetism (AFM) and charge-density-wave (CDW) order. We demonstrate that a simple picture of AFM-CDW competition that incorporates the phonon-mediated attraction into an effective-U Hubbard model requires significant refinement. Specifically, retardation effects slow the onset of charge order so that CDW order remains absent even when the effective U is negative. This delay opens a window where neither AFM nor CDW order is well established and where there are signatures of a possible metallic phase.

DOI: 10.1103/PhysRevLett.109.246404 PACS numbers: 71.10.Fd, 71.30.+h, 71.38.−k, 71.45.Lr

The electron-phonon (e-ph) interaction is responsible for many phenomena in condensed-matter physics, including charge-density waves (CDWs) and conventional superconductivity. While the e-ph interaction is well understood in metals, the role of phonons in strongly correlated systems is less clear, in part because the interplay of strong electron-electron (e-e) and e-ph interactions can lead to competing ordered phases. Despite its difficulty, this is an important problem to solve because multiple experimental probes have detected signatures of significant lattice effects in strongly correlated materials. For example, in the cuprate high-temperature superconductors, angle-resolved photoemission spectroscopy has observed ''kinks'' in the band dispersion, which have been attributed to the e-ph interaction [1], as well as small polaron formation in undoped $Ca_{2-x}Na_xCuOCl_2$ [2,3]. Additional evidence for a significant e-ph interaction includes strong quasiparticle renormalizations detected by STM [4] and studies that have qualitatively reproduced optical conductivity peaks by including phonons [5,6]. Besides the cuprates, other materials with both strong e-e and e-ph interactions include the manganites [7] and fullerenes [8].

On general grounds, two effects are expected when e-ph interactions are included in a system with strong e-e repulsion. The first is that the two interactions renormalize each other. The phonons mediate a retarded attractive e-e interaction, thus reducing the effective Coulomb repulsion, while the e-e repulsion suppresses charge fluctuations and, hence, the e-ph interaction, which couples to them. The second effect is a reduction in the quasiparticle weight due to additional scattering processes, which at large e-ph couplings can lead to a polaron crossover.

A natural model for studying the interplay of the e-e and e-ph interactions is the Hubbard-Holstein (HH) model, which has been studied using various numerical approaches producing sometimes contradictory results. Within dynamical mean field theory (DMFT), the suppression of the e-ph interaction depends on the underlying phase, and antiferromagnetic (AFM)-DMFT has found a moderate increase in the critical e-ph coupling for small polaron formation [9,10]. In contrast, diagrammatic quantum Monte Carlo work on the t-J-Holstein model found a reduction in the critical e-ph coupling needed for small polaron crossover [11]. Dynamical cluster approximation studies investigated the effect of phonons on the superconducting T_c and found that phonons suppress T_c at small doping levels [12]; however, including longer range hopping terms in the presence of phonons enhanced T_c [13].

In addition to renormalization effects arising from the interplay of the e-e and e-ph interactions, competition between ordered phases can occur. On a two-dimensional square lattice, at half filling the Hubbard and Holstein models have instabilities towards $(\pi/a, \pi/a)$ AFM and CDW orders, respectively; these phases compete in the HH model. Due to the many-body nature of the problem, compounded by the many degrees of freedom in the HH model, in general there is no exact solution. In one dimension, the HH phase diagram has been established via

several numerical approaches, with an intermediate metallic state between the AFM and CDW phases [14–18]. The size of the metallic region grows with increasing phonon frequency [15–17]. A similar competition between AFM and CDW orders and phase diagram has been mapped out in infinite dimensions with DMFT [19–23]. The AFM-CDW competition in two dimensions also has been studied with perturbative [24,25] as well as strong coupling [26] techniques.

In this Letter, we present a determinant quantum Monte Carlo (DQMC) study of the two-dimensional single-band HH model at half filling. DQMC is a numerically exact method that treats e-e and e-ph interactions on an equal footing and nonperturbatively. A nonzero e-ph coupling introduces the fermion sign problem at half filling [27]. Nevertheless, simulations for all parameter ranges presented in this work can be done down to $T = W/40$, where W is the noninteracting bandwidth. Significantly lower temperatures can be reached in some regimes. For details of the DQMC method, please refer to Refs. [28–30].

The Hamiltonian for the single-band HH model is $H = H_{\text{kin}} + H_{\text{lat}} + H_{\text{int}}$, where

$$H_{\text{kin}} = -t\sum_{\langle ij\rangle\sigma} c^{\dagger}_{i\sigma}c_{j\sigma} - \mu\sum_{i\sigma}\hat{n}_{i\sigma},$$
$$H_{\text{lat}} = \sum_i\left(\frac{M\Omega^2}{2}\hat{X}_i^2 + \frac{1}{2M}\hat{P}_i^2\right), \quad (1)$$
$$H_{\text{int}} = U\sum_i\left(\hat{n}_{i\uparrow} - \frac{1}{2}\right)\left(\hat{n}_{i\downarrow} - \frac{1}{2}\right) - g\sum_{i\sigma}\hat{n}_{i\sigma}\hat{X}_i.$$

Here, $\langle\ldots\rangle$ denotes a sum over nearest neighbors, $c^{\dagger}_{i\sigma}$ creates an electron with spin σ at site i, $\hat{n}_{i\sigma} = c^{\dagger}_{i\sigma}c_{i\sigma}$, t is the nearest neighbor hopping, Ω is the phonon frequency, U is the e-e interaction strength, g is the e-ph interaction strength, and μ is the chemical potential, which is adjusted to maintain half filling. The dimensionless electron-phonon coupling constant is defined as $\lambda = g^2/M\Omega^2W$. Throughout, we take $t = 1$, $M = 1$, and $a = 1$ as our units of energy, mass, and length, respectively.

We first study the spin and charge susceptibilities χ_s and χ_c, which are given by

$$\chi_{s,c}(\mathbf{q}) = \frac{1}{N}\int_0^{\beta} d\tau\langle T_\tau\hat{O}_{s,c}(\mathbf{q},\tau)\hat{O}^{\dagger}_{s,c}(\mathbf{q},0)\rangle, \quad (2)$$

where $\hat{O}_s(\mathbf{q}) = \sum_i e^{i\mathbf{q}\cdot\mathbf{R}_i}(\hat{n}_{i\uparrow} - \hat{n}_{i\downarrow})$, and $\hat{O}_c(\mathbf{q}) = \sum_i e^{i\mathbf{q}\cdot\mathbf{R}_i}(\hat{n}_{i\uparrow} + \hat{n}_{i\downarrow})$.

The susceptibilities at wave vector $\mathbf{q} = (\pi,\pi)$ are shown in Fig. 1 for several values of U. With increasing λ, χ_s decreases, signaling that the e-ph interaction reduces the strength of the effective e-e repulsion. This decrease in χ_s occurs immediately with the inclusion of nonzero λ for low to intermediate U, whereas for large U, suppression of χ_s does not occur until the e-ph coupling is fairly strong ($\lambda = 0.5$ for $U = 8t$ and $\lambda > 1$ for $U = 10t$). As χ_s shrinks, χ_c increases, indicating a clear competition

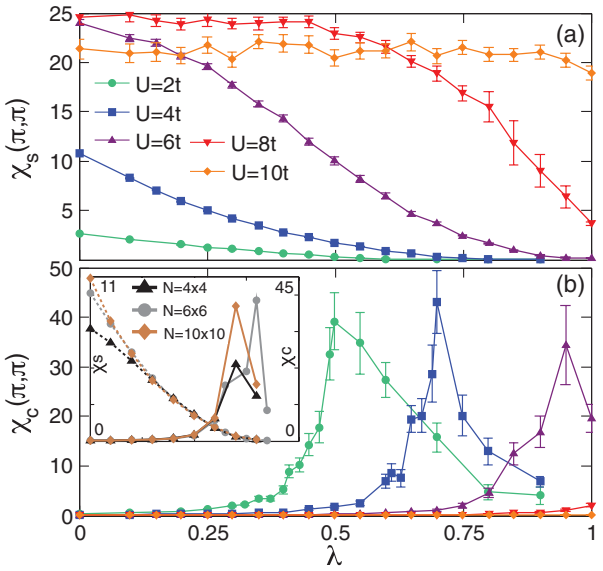

FIG. 1 (color). (a) $\chi_s(\pi,\pi)$ and (b) $\chi_c(\pi,\pi)$ for several U values on an $N = 8\times 8$ lattice. Inset of (b) shows χ_s (dashed lines) and χ_c (solid lines) at $U = 4t$ for several lattice sizes. The error bars in the inset are suppressed for clarity. The remaining simulation parameters are $\beta = 4/t$, $\Delta\tau = 0.1/t$, $\Omega = t$.

between the spin and charge orders. For all values of U considered here, χ_c is negligible up to a U-dependent critical λ, at which point it grows rapidly. However, for strong e-e interactions ($U = 8t$, $10t$), χ_c is still relatively small even at $\lambda = 1$, due to the strong tendency toward AFM still present. Interestingly, rather than continuously growing with λ, the CDW susceptibility peaks and then decreases, for $U = 2t$–$6t$. We attribute this behavior to the finite CDW transition temperature in the HH model, which will be discussed in more detail below. The inset in Fig. 1(b) shows χ_s and χ_c for $U = 4t$ for several lattice sizes, demonstrating that the lattice size has little effect on our conclusions.

Since one of the effects of e-ph coupling is to reduce the effective strength of U, we investigate how well a U_{eff} Hubbard model can describe the physics of the HH model. Integrating out the phonon field in the HH model yields a dynamic e-e interaction

$$U_{\text{eff}}(\omega) = U - \frac{g^2}{M(\Omega^2 - \omega^2)}. \quad (3)$$

In the antiadiabatic limit ($\Omega\to\infty$), this interaction becomes instantaneous and reduces to the form $U_{\text{eff}} = U - \lambda W$. A frequency-independent U_{eff} Hubbard model is often used to describe the HH model, even at finite Ω. For example, DMFT studies have found that such an approach captures the low-energy physics of the HH model [9,22].

Figure 2 compares the spin and charge structure factors $S_{s,c}(\mathbf{q}) = \langle\hat{O}_{s,c}(\mathbf{q})\hat{O}^{\dagger}_{s,c}(\mathbf{q})\rangle$ at $\mathbf{q} = (\pi,\pi)$ of a frequency-independent U_{eff} Hubbard model and the $U = 8t$ HH

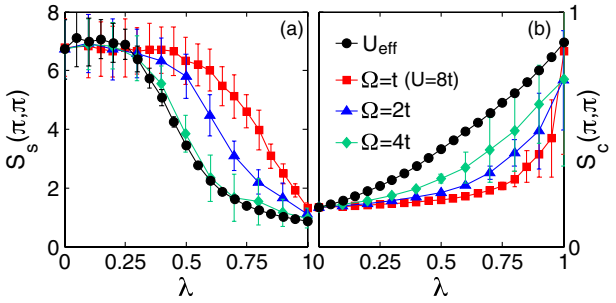

FIG. 2 (color online). Structure factors (a) $S_s(\pi, \pi)$ and (b) $S_c(\pi, \pi)$ for a U_{eff} Hubbard model (black) and the $U = 8t$ HH model with several phonon frequencies. The remaining simulation parameters are $N = 8 \times 8$, $\beta = 4/t$, $\Delta\tau = 0.1/t$.

model at several phonon frequencies. Up to $\lambda \approx 0.25$, $S_s(\pi, \pi)$ in the U_{eff} and HH models agrees for all Ω considered. Beyond this point, $S_s(\pi, \pi)$ is suppressed more slowly in the HH model than in the U_{eff} model, due to the retarded nature of the e-ph interaction captured in HH. As Ω increases, the HH result comes closer to the U_{eff} result, until by $\Omega = 4t$, the two models agree within the error bars. We also considered other values of U (not shown) and found that for a given Ω the difference between the HH and U_{eff} results grows as U increases. In contrast to $S_s(\pi, \pi)$, $S_c(\pi, \pi)$ calculated in the U_{eff} and HH models does not agree for any λ. Rather, $S_c(\pi, \pi)$ immediately rises in the U_{eff} model, whereas in the HH model it remains small until $\lambda \approx 0.75$ and then rises sharply. As the phonon frequency increases, the HH and U_{eff} results get closer, although they are still inconsistent at $\Omega = 4t$. This result is generic; while the U_{eff} Hubbard model has a CDW phase for any U_{eff} that is negative, χ_c remains suppressed well beyond the λ value at which $U_{\text{eff}} = 0$, as is clear in Fig. 1(b) where $U_{\text{eff}} = 0$ at $\lambda = 0.25$, 0.5, and 0.75 for $U = 2t$, $4t$, and $6t$, respectively.

An additional difference between the HH and U_{eff} models is the CDW transition temperature. In the HH model, while $T_{\text{AFM}} = 0$ in two dimensions due to the Mermin-Wagner theorem, T_{CDW} is finite because the order parameter has two states. DQMC finite size scaling studies [31,32] of the Holstein model found that $t\beta_{\text{CDW}} = 8$–11 for $\Omega = t$ and $\lambda = 0.25$. While we did not perform a scaling analysis for the HH model, we expect T_{CDW} to be in the same temperature regime, because while the inclusion of U in the HH model localizes carriers (which would lower T_{CDW}), it also pushes the CDW transition to a larger λ (which would increase T_{CDW}). In contrast, $T_{\text{CDW}} = 0$ in the attractive-U Hubbard model. The sharply peaked nature of χ_c in Fig. 1(b), differing from the slow evolution of χ_s, may be due to the proximity of the temperature $t\beta = 4$ to T_{CDW}.

We now turn to the spectral properties of the HH model. To avoid analytic continuation, we focus on the spectral weight near the Fermi level, which is obtained from the imaginary time propagator via the relation [33]

$$\beta C(\mathbf{k}, \tau = \beta/2) = \frac{\beta}{2} \int d\omega A(\mathbf{k}, \omega) g(\omega, \beta), \quad (4)$$

where C and A are the propagator and spectral function, respectively, and $g(\omega, \beta) = \omega/\sinh(\beta\omega/2)$ for bosons and $= 1/\cosh(\beta\omega/2)$ for fermions. At low temperature, $g(\omega, \beta)$ is sharply peaked about $\omega = 0$, so that $A(\mathbf{k}, \omega = 0)$ dominates the integral. We consider the local propagator $C(\mathbf{r} = 0) = \sum_{\mathbf{k}} C(\mathbf{k})$, which is related to the low-energy projected density of states via $N(0) \approx \beta C(\mathbf{r} = 0, \tau = \beta/2)/\pi$.

The phonon propagator, defined as $D_{ij}(\tau) = \langle T_\tau \hat{X}_i(\tau)\hat{X}_j(0)\rangle - \langle X\rangle^2$, contains information on phonon softening at the CDW transition. In the Holstein model, the phonon spectral function is peaked at the bare phonon frequency $\pm\Omega$ in a system without e-ph coupling; e-ph interactions renormalize the phonon frequency and lead to spectral weight at other frequencies. In particular, the appearance of spectral weight at $\omega = 0$ indicates the development of a static CDW lattice distortion, which is revealed by $\beta D(\mathbf{r} = 0, \tau = \beta/2)$ (abbreviated as $\beta D_{\beta/2}$), as shown in Fig. 3. For low e-ph coupling, $\beta D_{\beta/2}$ is negligible, since the system is far from the CDW state. It then increases at the same U-dependent λ at which χ_c rapidly increases in Fig. 1(b). This phonon softening indicates that the CDW formation may have a Peierls-like origin, in which case the Fermi surface could be restored during the transition from an AFM to a CDW insulator. Figure 3(b) shows χ_c at $U = 2t$ for several lower temperatures. With decreasing temperature, the rise in χ_c sharpens dramatically and also shifts to lower λ, appearing to asymptote towards a divergence in the susceptibility at low temperature around $\lambda = 0.3$. We also note that the peak and subsequent decay in the CDW susceptibility discussed earlier appears robustly as a function of temperature.

The electronic spectral weight near $\omega = 0$ also offers insight into the AFM-CDW transition. In this case, $\beta G(\mathbf{r} = 0, \tau = \beta/2)$ (abbreviated as $\beta G_{\beta/2}$) distinguishes between insulating and metallic systems, being 0 in the

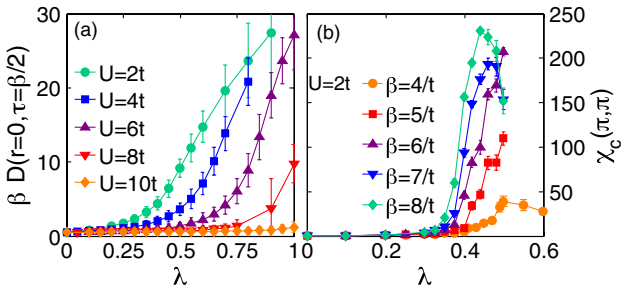

FIG. 3 (color online). (a) Local phonon propagator $\beta D(\mathbf{r} = 0, \tau = \beta/2)$ for several values of U at $\beta = 4/t$. (b) $\chi_c(\pi, \pi)$ for $U = 2t$ and several values of β. The remaining simulation parameters are $N = 8 \times 8$, $\Delta\tau = 0.1/t$, $\Omega = t$.

low-temperature limit when a gap is present and finite if a band disperses through the Fermi level. Figure 4(a) shows $\beta G_{\beta/2}$ for several values of U. For small λ values, $\beta G_{\beta/2}$ decreases with increasing U, indicating the opening of the Mott gap. As a function of increasing λ, $\beta G_{\beta/2}$ falls for $U = 2t$ as the CDW gap develops. For $U = 4t$ and $6t$, $\beta G_{\beta/2}$ initially grows as the e-ph interaction reduces the effective e-e repulsion and the Mott gap closes and then decreases quickly as the CDW gap opens. For all these U values, $\beta G_{\beta/2}$ begins to fall at the same λ at which χ_c increases in Fig. 1(b) and the phonon softens in Fig. 3(a). For $U = 8t$ and $10t$, $\beta G_{\beta/2}$ grows slowly with λ as the Mott gap narrows.

What can the peak in $\beta G_{\beta/2}$ at intermediate λ in Fig. 4(a) tell us about the AFM-CDW transition? In Fig. 4(b), we plot $\beta G_{\beta/2}$ at $U = 5t$ for several temperatures. As the temperature is lowered, $\beta G_{\beta/2}$ decreases at small and large λ as the Mott and CDW gaps open, respectively. However, at intermediate e-ph coupling, $\beta G_{\beta/2}$ actually grows with decreasing temperature, behavior that could arise from an intervening metallic phase between the Mott and CDW insulating states. This increase in spectral weight at intermediate λ was observed robustly for several lattice sizes and values of U. In addition, the possible implication of a Fermi surface in the intermediate state, from the phonon softening in Fig. 3(a), further supports the idea of an intermediate metallic phase.

To further explore signatures of this possible metallic state, we plot the average double occupancy $\langle n_\uparrow n_\downarrow \rangle$ in Fig. 4(c). The double occupancy distinguishes between (π, π) AFM and CDW insulators, where it is 0 and 0.5, respectively. In a metallic state (or an AFM-CDW coexistence state), $\langle n_\uparrow n_\downarrow \rangle = 0.25$. We find that $\langle n_\uparrow n_\downarrow \rangle$ increases smoothly with energy through 0.25, which is consistent with an intermediate metallic state, rather than a direct AFM-CDW transition at a critical λ value, where a sharp jump would be expected. While the transition from low to high double occupancy may sharpen as temperature is lowered, we note that in the range $t\beta = 2$–5, we found much less temperature dependence in $\langle n_\uparrow n_\downarrow \rangle$ than in other quantities considered in this Letter.

A finite temperature $U - \lambda$ phase diagram for $\beta = 4/t$, depicting the difference of the charge and spin order parameters, $\Phi_c - \Phi_s$, is shown in Fig. 4(d). Here, the order parameters are defined as $\Phi_s = \sum_i (\hat{n}_{i\uparrow} - \hat{n}_{i\downarrow})^2/N$ and $\Phi_c = \sum_{i\sigma} (\hat{n}_{i\sigma} - 1)^2/N$. Lines denoting $U_{\text{eff}} = 0$, $\langle n_\uparrow n_\downarrow \rangle = 0.25$, and the peak in $\beta G_{\beta/2}$ are also included. The dominance of AFM and CDW orders at large U and λ values, respectively, is apparent. However, a sizable transition region, where $\Phi_c - \Phi_s \approx 0$, is clearly visible. The lines $U_{\text{eff}} = 0$ and $\langle n_\uparrow n_\downarrow \rangle = 0.25$ lie in the center of the transition region, while the peak in $\beta G_{\beta/2}$ is toward the side dominated by spin order. The coincidence of multiple quantities consistent with a metallic state in the intermediate region of the phase diagram corroborates the case for the existence of such a phase.

To summarize, in this work we demonstrated a strong competition between AFM and CDW phases in the

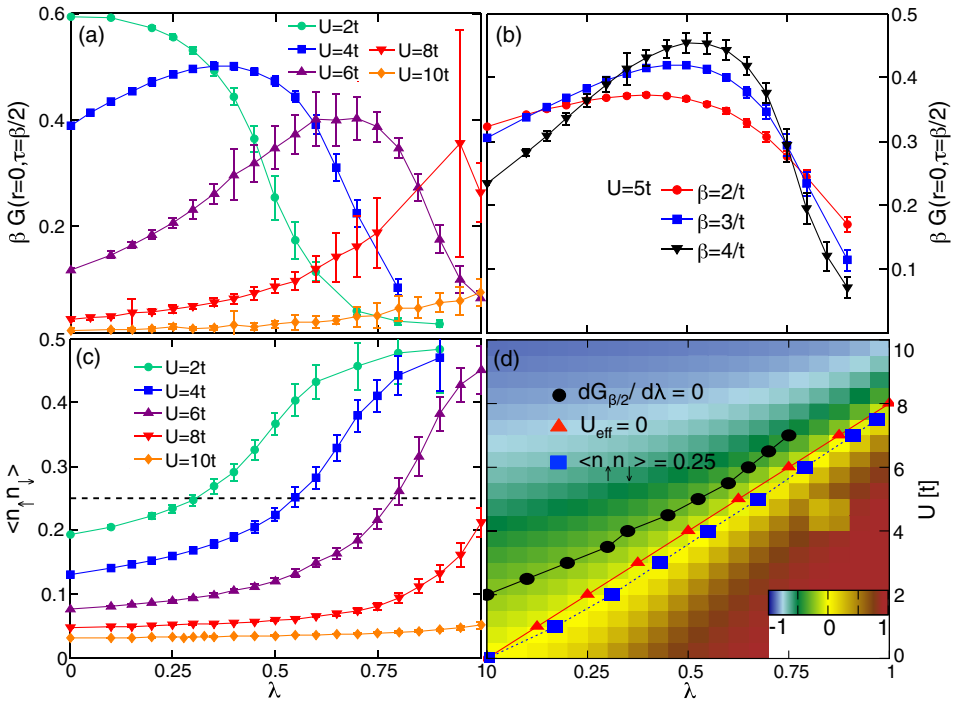

FIG. 4 (color online). Local electron Green's function $\beta G(\mathbf{r} = 0, \tau = \beta/2)$ for (a) several values of U at $\beta = 4/t$ and (b) at $U = 5t$ for several β. (c) Average double occupancy $\langle n_\uparrow n_\downarrow \rangle$ at $\beta = 4/t$. The dashed line indicates where $\langle n_\uparrow n_\downarrow \rangle = 0.25$. (d) $\Phi_c - \Phi_s$ at $\beta = 4/t$. The remaining simulation parameters are $N = 8 \times 8$, $\Delta\tau = 0.1/t$, $\Omega = t$.

two-dimensional single band HH model and found evidence for a possible intermediate metallic regime existing between the ordered phases. We investigated how well an effective-U Hubbard model can describe the physics of the HH model and found that while in some regimes the two models give comparable results, in general the retarded nature of the e-ph interaction leads to significant differences. The $U - \lambda$ phase diagram determined in our study is qualitatively similar to that found by low-temperature numerical approaches, with the $U_{\text{eff}} = 0$ line dividing the regions of dominant spin and charge order parameters. We found evidence for an intermediate metallic phase in two dimensions, similar to that of previous 1D results [14–17]. The size of the intermediate metallic region shrinks as the interaction strengths grow, which is consistent with Refs. [15–17], where the metallic phase is found to terminate at strong couplings. These findings contrast with the infinite dimensional DMFT results of Refs. [22,23], where a direct order-to-order transition was found. Potential explorations for future work include studying the effect of phonon frequency on the intermediate metallic state and understanding more precisely where the metal-insulator transitions lie.

E. A. N. and S. J. contributed equally to this work. We thank N. Nagaosa and A. S. Mishchenko for useful discussions. We acknowledge support from the U.S. Department of Energy, Office of Basic Energy Sciences, Materials Science and Engineering Division under Contracts No. DE-AC02-76SF00515 and No. DE-FC0206ER25793. E. A. N. acknowledges support from EAPSI and S. J. acknowledges support from SHARCNET and NSERC.

[1] A. Lanzara, P. V. Bogdanov, X. J. Zhou, S. A. Kellar, D. L. Feng, E. D. Lu, T. Yoshida, H. Eisaki, A. Fujimori, K. Kishio *et al.*, Nature (London) **412**, 510 (2001).
[2] K. M. Shen, F. Ronning, D. H. Lu, W. S. Lee, N. J. C. Ingle, W. Meevasana, F. Baumberger, A. Damascelli, N. P. Armitage, L. L. Miller *et al.*, Phys. Rev. Lett. **93**, 267002 (2004).
[3] K. M. Shen, F. Ronning, W. Meevasana, D. H. Lu, N. J. C. Ingle, F. Baumberger, W. S. Lee, L. L. Miller, Y. Kohsaka, M. Azuma *et al.*, Phys. Rev. B **75**, 075115 (2007).
[4] J. Lee, K. Fujita, K. McElroy, J. A. Slezak, M. Wang, Y. Aiura, H. Bando, M. Ishikado, T. Masui, J.-X. Zhu *et al.*, Nature (London) **442**, 546 (2006).
[5] A. S. Mishchenko, N. Nagaosa, Z.-X. Shen, G. De Filippis, V. Cataudella, T. P. Devereaux, C. Bernhard, K. W. Kim, and J. Zaanen, Phys. Rev. Lett. **100**, 166401 (2008).
[6] G. De Filippis, V. Cataudella, A. S. Mishchenko, C. A. Perroni, and N. Nagaosa, Phys. Rev. B **80**, 195104 (2009).
[7] A. J. Millis, Nature (London) **392**, 147 (1998).
[8] P. Durand, G. R. Darling, Y. Dubitsky, A. Zaopo, and M. J. Rosseinsky, Nat. Mater. **2**, 605 (2003).
[9] G. Sangiovanni, M. Capone, C. Castellani, and M. Grilli, Phys. Rev. Lett. **94**, 026401 (2005).
[10] G. Sangiovanni, O. Gunnarsson, E. Koch, C. Castellani, and M. Capone, Phys. Rev. Lett. **97**, 046404 (2006).
[11] A. S. Mishchenko and N. Nagaosa, Phys. Rev. Lett. **93**, 036402 (2004).
[12] A. Macridin, B. Moritz, M. Jarrell, and T. Maier, Phys. Rev. Lett. **97**, 056402 (2006).
[13] E. Khatami, A. Macridin, and M. Jarrell, Phys. Rev. B **78**, 060502 (2008).
[14] Y. Takada and A. Chatterjee, Phys. Rev. B **67**, 081102 (2003).
[15] R. T. Clay and R. P. Hardikar, Phys. Rev. Lett. **95**, 096401 (2005).
[16] R. P. Hardikar and R. T. Clay, Phys. Rev. B **75**, 245103 (2007).
[17] H. Fehske, G. Hager, and E. Jeckelmann, Europhys. Lett. **84**, 57001 (2008).
[18] H. A. Craig, C. N. Varney, W. E. Pickett, and R. T. Scalettar, Phys. Rev. B **76**, 125103 (2007).
[19] W. Koller, D. Meyer, Y. Ono, and A. C. Hewson, Europhys. Lett. **66**, 559 (2004).
[20] W. Koller, D. Meyer, and A. C. Hewson, Phys. Rev. B **70**, 155103 (2004).
[21] P. Werner and A. J. Millis, Phys. Rev. Lett. **99**, 146404 (2007).
[22] J. Bauer, Europhys. Lett. **90**, 27002 (2010).
[23] J. Bauer and A. C. Hewson, Phys. Rev. B **81**, 235113 (2010).
[24] S. Kumar and J. van den Brink, Phys. Rev. B **78**, 155123 (2008).
[25] E. Berger, P. Valášek, and W. von der Linden, Phys. Rev. B **52**, 4806 (1995).
[26] T. Hotta and Y. Takada, Phys. Rev. B **56**, 13916 (1997).
[27] S. Johnston, Ph.D. thesis, University of Waterloo, 2010, http://hdl.handle.net/10012/5274.
[28] R. Blankenbecler, D. J. Scalapino, and R. L. Sugar, Phys. Rev. D **24**, 2278 (1981).
[29] S. R. White, D. J. Scalapino, R. L. Sugar, E. Y. Loh, J. E. Gubernatis, and R. T. Scalettar, Phys. Rev. B **40**, 506 (1989).
[30] R. T. Scalettar, N. E. Bickers, and D. J. Scalapino, Phys. Rev. B **40**, 197 (1989).
[31] R. M. Noack, D. J. Scalapino, and R. T. Scalettar, Phys. Rev. Lett. **66**, 778 (1991).
[32] M. Vekić, R. M. Noack, and S. R. White, Phys. Rev. B **46**, 271 (1992).
[33] N. Trivedi and M. Randeria, Phys. Rev. Lett. **75**, 312 (1995).